

Atom Interferometry with up to 24-Photon-Momentum-Transfer Beam Splitters

Holger Müller,^{1,*} Sheng-wei Chiow,¹ Quan Long,^{1,†} Sven Herrmann,¹ and Steven Chu^{1,2}

¹*Physics Department, Stanford University, 382 Via Pueblo Mall, Stanford, California 94305, USA*

²*Lawrence Berkeley National Laboratory and Department of Physics, University of California, Berkeley, 1 Cyclotron Road, Berkeley, CA 94720.*

(Dated: October 26, 2018)

We present up to 24-photon Bragg diffraction as a beam splitter in light-pulse atom interferometers to achieve the largest splitting in momentum space so far. Relative to the 2-photon processes used in the most sensitive present interferometers, these large momentum transfer beam splitters increase the phase shift 12-fold for Mach-Zehnder (MZ-) and 144-fold for Ramsey-Bordé (RB-) geometries. We achieve a high visibility of the interference fringes (up to 52% for MZ or 36% for RB) and long pulse separation times that are possible only in atomic fountain setups. As the atom's internal state is not changed, important systematic effects can cancel.

PACS numbers: 03.75.Dg, 37.25.+k, 67.85.-d

Light-pulse atom interferometers are tools for experiments of exquisite precision [1], such as tests of general relativity [2] and measurements of the fine-structure constant α [3, 4, 5], the local gravitational acceleration g [6], its gradient [7], the Sagnac effect [8], or Newton's gravitational constant [9]. Their sensitivity compares favorably with the best competing methods. Substantial progress would not only improve the above experiments, but also enable new ones: For example, tests of gravity [10], quantum electrodynamics [11], or the detection of gravitational waves [12]. Like in optical interferometers, the sensitivity scales with the phase difference ϕ of the waves in the interferometer arms. This can be increased via the arms' momentum-space splitting. Conventionally, the splitting is provided by the momentum of $2\hbar k$ that is transferred to the atom by a two-photon process (where k is the wavenumber). Efforts to increase it have been limited to $6\hbar k$. They have used momentum transfer by extra light pulses [13, 14], which might lead to additional systematic effects, or supersonic atomic beams [15, 16], whose inherently short evolution time limits the sensitivity. Up to $140\hbar k$ have been transferred by adiabatic transfer [3, 4], but this affects the common, not the relative momentum of the arms. Here, we use multiphoton Bragg diffraction of atoms by an optical lattice as a beam splitter. We achieve interferometry with a momentum-space splitting of up to $24\hbar k$, the largest so far. In some important applications [3, 4, 11], this leads to a 144-fold increase in the phase. Moreover, Bragg diffraction does not change the atom's internal state, so that important systematic effects can cancel. This work thus allows for substantial progress in both sensitivity and precision of atom interferometry.

In multiphoton Bragg diffraction, the atom coherently scatters $2n$ photons from a pair of antiparallel

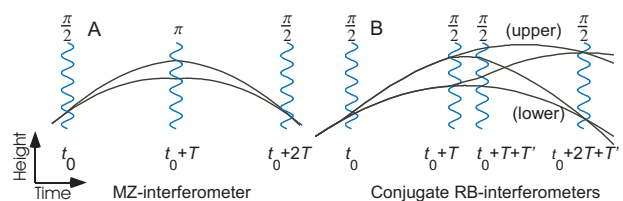


FIG. 1: A: MZI. “ $\pi/2$ ” pulses transfer momentum with a probability of 1/2. They thus act as beam splitters; “ π ” pulses act as mirrors. B: Conjugate RBIs; either is selected by the last $\pi/2$ pulse pair as described in the text. Not shown are outputs of the third beam splitter, which do not interfere.

laser beams, without changing its internal state. The atom thereby acquires a kinetic energy of $4n^2\hbar\omega_r$, where $\omega_r = \hbar k^2/(2M)$ is the recoil frequency and M the mass of the atom. Match with the energy $n\hbar(\omega_1 - \omega_2)$ lost by the laser field defines the resonance condition for the difference frequency $\omega_1 - \omega_2$ of the beams. Bragg diffraction has been used to transfer up to $16\hbar k$ [17], but interferometry so far has been limited to $6\hbar k$ [15, 16], with up to 26% visibility of the interference fringes [16]. These atomic beam setups are also limited by a relatively short pulse separation time of < 1 ms.

The phase difference $\phi = \phi_F + \phi_I$ contains a contribution of the atom's evolution between the beam splitters ϕ_F , and one of their interaction ϕ_I . To discuss specifically the effects of large momentum transfer beam splitters, it is useful to consider Mach-Zehnder and Ramsey-Bordé interferometers (MZI and RBI) separately. In MZIs (Fig. 1 A), ϕ_F vanishes for constant g , but gravity causes a ϕ_I by lowering the height at which the arms interact with the beam splitters. If the momentum transferred by the beam splitter is $2n\hbar k$, where n is an integer, a MZI thus has a phase difference of [1, 6] $\phi_{\text{MZ}} = n(2kgT^2 - \phi_L)$, where $\phi_L = \phi_1 - 2\phi_2 + \phi_3$ are the phases ϕ_{1-3} of the laser fields at some reference point. Here, multiphoton beam splitters lead to a linear increase in phase. In RBIs, only one arm receives momentum from the beam splitters (Fig. 1 B). Thus, $\phi_F = 2E_{\text{kin}}T/\hbar$ is

*Electronic address: holgerm@stanford.edu

†Now at Physics Department, Huazhong University of Science and Technology, Wuhan 430074, Hubei, China.

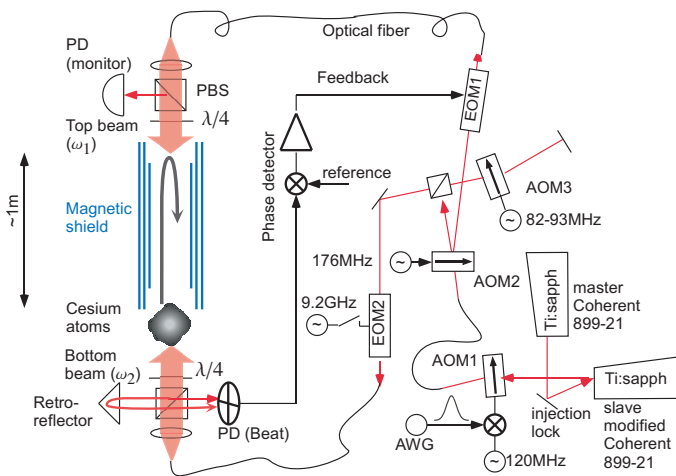


FIG. 2: Setup (simplified). PD; photodetector. For the injection lock, we use polarization spectroscopy [18], which does not require modulation of the laser light. AOM1 (Isomet 1206C) amplitude modulates, AOM2 (Crystal Technology 3200-124) splits and AOM3 (Isomet 1205C-1) ramps the frequency of the beams. EOM2 (New Focus) generates ~ 9.2 GHz sidebands for the velocity selection.

nonzero due to the difference in kinetic energy E_{kin} . The same term, times minus two, enters ϕ_I due to the modified locations at which the atoms interact. Summing up, [4]

$$\phi_{\text{RB}} = \pm 8n^2\omega_r T + 2nkg(T + T')T + n\phi_L. \quad (1)$$

The plus and minus signs are for the upper and lower interferometer, respectively, and $\phi_L = \phi_2 - \phi_1 - \phi_4 + \phi_3$ is given by the phases ϕ_{1-4} of the laser pulses. The recoil term in RBIs scales quadratically with the momentum splitting. So far, the highest was $4\hbar k$. It has been achieved by applying additional light pulses [14].

Our apparatus (Fig. 2) loads ^{133}Cs atoms from a 2-dimensional magneto-optical trap (2D-MOT; not shown) into a 3D-MOT. A moving optical molasses accelerates them upwards (“launches”) to a 1-m high, 0.9-s ballistic trajectory, at a temperature of $1.2 - 2 \mu\text{K}$. Doppler-sensitive Raman transitions driven by the top and bottom beams select $\sim 10^6$ atoms in the $6S_{1/2}$, $F = 3$, $m_F = 0$ state with a narrowed vertical velocity distribution of about $0.3 v_r$ full width at half maximum (FWHM). Here, $v_r = \hbar k/M \simeq 3.5 \text{ mm/s}$ is the recoil velocity for a wavelength of 852 nm (the Cs D2 line).

High-powered laser beams are mandatory for driving high-order multiphoton Bragg diffraction. On the one hand, the effective Rabi frequency [19, 20] $\Omega_{\text{eff}} \approx \Omega^n / [(8\omega_r)^{n-1} (n-1)!^2]$ is a very strong function of the 2-photon Rabi frequency Ω , i.e., of laser intensity. On the other hand, beams of large radius are required to accommodate the spread of the sample. To generate the required power, we use a system of injection-locked Ti:sapphire lasers (Fig. 2). A first ~ 1.2 -W Ti:sapphire laser is frequency stabilized (“locked”) to the $6S_{1/2}$,

$F = 3 \rightarrow 6P_{3/2}$, $F = 4$ transition in a Cs vapor cell, with a blue detuning δ of 0-20 GHz set by a microwave synthesizer. It injection locks a second one, which has no intracavity etalons or Brewster plate, and an output coupler with 10% transmission (CVI part No. PR1-850-90-0537). Pumped with 17 – 19 W from a Coherent Innova 400 argon-ion laser, it provides a single-frequency output power of up to 6 W, about 2 times more than the strongest previously reported [21].

Acousto-optical modulators (AOMs) split the laser light into the top and bottom beams and shape them into Gaussian pulses, defined by arbitrary waveform generators (AWGs). Due to the free fall of the atoms, the resonance condition for $\omega_1 - \omega_2$ changes at a rate of 23 MHz/s, which we account for by continuously ramping $\omega_1 - \omega_2$ at a rate of r by AOM3. The ramp (provided by an Analog Devices AD9954 synthesizer) has a step size of $\sim 0.01 \mu\text{s}$, i.e., is essentially smooth even on the time-scale of a single Bragg pulse.

Coherent Bragg diffraction at high order n requires proportionally lower optical wavefront distortions. To reduce random aberrations, we minimize the number of optical surfaces. The beams reach the experiment via 5-m long, single-mode, polarization maintaining fibers and are collimated at a $1/e^2$ intensity radius of 8.6 mm by a doublet lens featuring low spherical aberration. Polarization is cleaned by 2” polarizing beam splitter (PBS) cubes and converted to $\sigma^+ - \sigma^+$ by zero-order $\lambda/4$ retardation plates having a specified $\lambda/20$ flatness.

For coherent high order Bragg diffraction, the beams also need to have exceptionally low phase fluctuations between the top and bottom beams. Therefore, we use a secondary phase lock [11, 22]: The phase is measured by detecting the beat note (Fig. 2) and compared to an electronic reference. Feedback is applied to EOM1 (New Focus 4002) via a fast high-voltage amplifier [23]. The ~ 100 ns response of this feedback loop allows us to re-lock at the beginning of each pulse, within a time that is negligible compared to the pulse length. The lock point relative to the reference will be the same for each pulse, modulo 2π , thus keeping the phase controlled within and in between pulses.

The performance of Bragg beam splitters depends critically on the choice of the duration, envelope function, and intensity of the pulses [19]. Our setup offers superior control of these. Short pulses, with their large Fourier width, reduce the sensitivity to the velocity spread of the atomic sample. However, below an FWHM of $n^{1/6} / [\omega_r (n-1)]$ for Gaussian pulses, losses into other diffraction orders become significant [19]. We use about $30 - 45 \mu\text{s}$. At a detuning of 750 MHz and a peak intensity of 0.5 W/cm^2 at the center of each beam, $30\hbar k$ momentum transfer was achieved at $> 50\%$ efficiency.

For MZ interferometry, we increase the detuning to $\delta = 4 \text{ GHz}$ to further reduce single-photon processes. We generally apply the first Bragg pulse about 100-200 ms after launch, when the thermal spread of the cloud is still negligible against the radius of the Bragg beams.

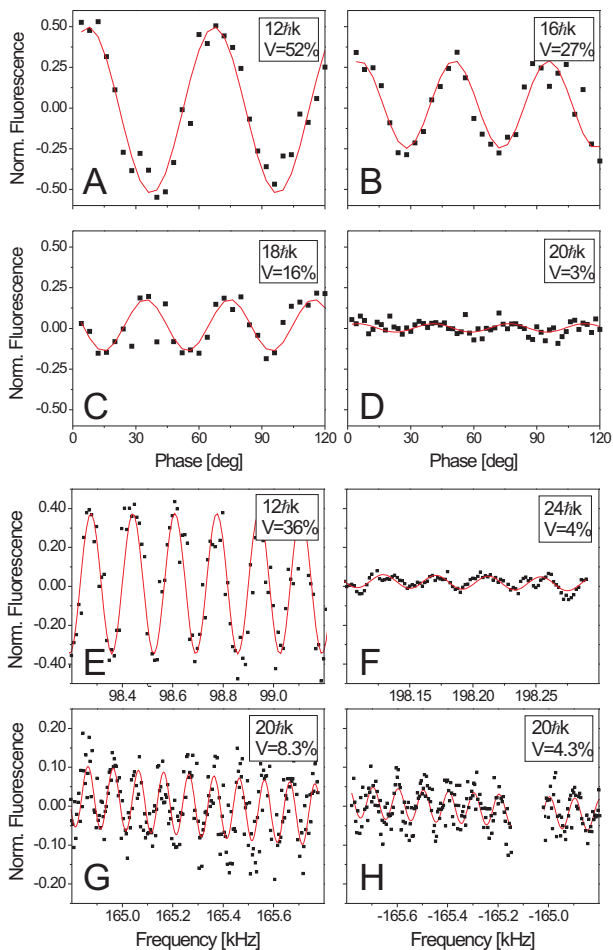


FIG. 3: A-D show MZI fringes with between 12 and $20\hbar k$ momentum transfer; E and F are RB fringes with 12 and $24\hbar k$. G and H show a conjugate $20\hbar k$ RB-pair. Throughout, $T = 1$ ms, $T' = 2$ ms. Each data point is from a single launch (that takes 2 s), except for F, where 5-point adjacent averaging was used. The lines represent a sinewave fit.

For $\leq 18\hbar k$ momentum transfer, we achieve a π -pulse efficiency of 80-90%. The fluorescence $f_{1,2}$ of the two interferometer outputs is detected as they pass a Hamamatsu R943-02 photomultiplier tube (located below the magnetic shield in Fig. 2). To take out fluctuations of the initial atom number, we use the normalized fluorescence $f = (f_1 - f_2)/(f_1 + f_2)$. We define the amplitude of a sinewave fit of the measured fringes as the visibility V . Fig. 3, A-D show fringes of MZIs with 12 to $20\hbar k$ momentum transfer, measured by scanning the phase of the last beam splitter. The period of the fringes is $2\pi/n$. Even at high orders, excellent visibility is achieved, like $V = 52\%$ at $12\hbar k$. The strong decrease of V at $20\hbar k$ is due to insufficient laser intensity to drive higher-order multi-photon transitions at $\delta = 4$ GHz.

For RBIs, we select the upper interferometer (Fig. 1 B), by shifting $\omega_1 - \omega_2$ of the last pulse pair by $\omega_u \simeq -8n\omega_r$, to meet the resonance condition for addressing the upper interferometer arms. As $\phi_L = rT^2 + \omega_u T$

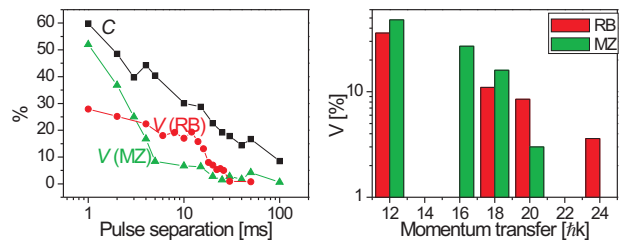


FIG. 4: Left: C and V (MZ) of $12\hbar k$ MZIs. V (RB) shows larger visibility at longer times for a RBI with vibration isolation (Minus K Technology Model 40BM1) for the lower beam and beat optics (Fig. 2). Right: Visibility versus momentum transfer.

(where $r \simeq 2\pi \times 23$ MHz/s is the ramp rate), we measure the interference fringes by scanning ω_u , see Fig. 3 E-H. Like for MZIs, we achieve an excellent visibility, e.g., $V = 36\%$ at $12\hbar k$. This is 72% of the theoretical maximum, which is $V = 50\%$ because each interferometer output overlaps with a fraction of the initial population, which does not interfere (Fig. 1 B). By reducing δ to 3.3 GHz, we can even increase the momentum transfer to $24\hbar k$ and achieve $V = 3.6\%$, which is still useful. Note that the period of the fringes is $1/(nT)$. Since additionally $\omega_u \propto n$, the resolution to which ω_r can be measured increases by n^2 , as expected.

Choosing an appropriate positive frequency shift ω_ℓ for the last $\pi/2$ pair forms a $20\hbar k$ lower RBI (Fig. 3 H). The contrast of this is somewhat reduced, as background atoms that could not be diffracted by the Bragg pulses overlap with one of the outputs. From a pair of conjugate RBIs, which use the same T and T' , $\omega_r = (\omega_\ell - \omega_u)/(16n)$ can be obtained independent of g , r , T , or T' . Here ω_ℓ, ω_u denote the values at the centers of the fringes.

The visibility decreases for long T and high n (Fig. 4). This may be ascribed to single-photon excitation (large n requires larger intensity), or thermal motion, which removes the atoms from the center of the Bragg beams, or wavefront distortions of the Bragg beams that smear out the phase over the atomic sample. Moreover, in spite of the secondary phase lock, phase noise enters in the atoms's inertial frame as a result of the vibrations of the laboratory frame, in which the phase is stabilized. At long T (where the vibrations are harder to isolate), the interferometers' phase thus becomes uncontrolled. Thus, the normalized fluorescence will fluctuate with a contrast $C = \sqrt{2}\sigma$, where σ is the standard deviation, but V goes to zero. From the measurement of C (Fig. 4) we find that, while V is reduced by vibrational noise, interference is still taking place throughout to a pulse separation time as long as $T = 100$ ms.

This work provides a tool for measurements of increased sensitivity and accuracy. For example, the fine-structure constant can be measured via the relation $\alpha^2 = (2R_\infty/c)(M/m_e)(h/M)$. The Rydberg constant R_∞ and the Cs to electron mass ratio M/m_e are known to precisions of 0.007 and 0.5 ppb, respectively [24]. A

non-interferometric measurement based on ~ 450 Bloch oscillations [5] and an RBI with 30 additional π pulses [4] both reach around 7 ppb in α . Replacing the beam splitters by 24 photon Bragg diffraction as demonstrated here can increase the phase of the RBI by a factor of 144. For example, from data taken with $n = 10$ (Fig. 3 G and H), we obtain $\omega_r = 2\pi \times 2066.427(11)$ Hz and $\alpha^{-1} = 137.03653(35)$ [2.6 ppm], compatible at 1.5σ with the accepted value. This statistical uncertainty would be 260 ppm if we had taken this data [$T = 1$ ms, $V \sim (4 - 10)\%$] with $n = 1$. While not being a competitive measurement of α , this clearly shows the power of the method.

We expect to increase T to 400 ms with the help of the vibration cancellation afforded by simultaneous conjugate RBIs [11, 22]. As the sensitivity scales like n^2T , use of $n = 12$ and $T = 400$ ms offers a ~ 500 -fold gain over the best previous RBI, ($n = 1, T = 120$ ms). Since the ultimate limit on the accuracy will be systematics, such a large sensitivity is unnecessary; operation without the 30 additional π pulses would still be sufficiently sensitive and help to reduce systematic effects by simplifying the geometry to a basic RBI. This has an additional benefit: the finite efficiency of the additional π pulses reduces the contrast to about 15% in Ref. [4]. With multiphoton Bragg diffraction, operation without additional π pulses is possible, which can make up for the loss of contrast at the highest Bragg diffraction orders (Figs. 3,4).

Moreover, Bragg diffraction leaves the internal quantum states of the atoms unchanged, so that systematic effects like the Zeeman and Stark effects cancel out between the interferometer paths. (A smaller contribution due to background field gradients remains.) The thick Bragg beams with good wavefront quality used here reduce other dominant systematic effects [3, 4, 5], while

the 80 μ rad phase noise of our laser system means that the final accuracy can be reached within low integration time. For other systematic effects and their suppression, see also [11, 22, 25]. A ppb-level measurement of α via \hbar/M could serve for testing of quantum electrodynamics by comparison to α as derived (to 0.4 ppb) from a measurement of the electron's anomalous magnetic moment $g - 2$ [26]. The influence of hadronic vacuum polarization would be revealed, and bounds on low energy dark matter and a possible internal structure of the electron could be established via their hypothetical effect on $g - 2$.

We have presented atom interferometers that use Bragg diffraction for beam splitters that transfer up to $24\hbar k$. Even with high ($12\hbar k$) momentum transfer, the visibility is comparable or superior to typical interferometers based on 2-photon transitions. Interference is observed up to a pulse separation of 100 ms. Up to $30\hbar k$ were transferred in a single diffraction. Factors that lead to this progress include (i) improved understanding of multiphoton Bragg diffraction [19], especially of the influence of the pulse shape, (ii) a 6-W injection locked Ti:sapphire laser system, (iii) good wavefront quality and large diameter of the Bragg beams, and (iv) a secondary phase locked loop to reduce phase noise. We have discussed applications for precision atom interferometry. The potential of multiphoton Bragg diffraction for atom interferometry is clear.

Many thanks to A. Peters and A. Senger for valuable help and to E. Sarajlic and N. Gemelke for discussions. This work was supported by the National Science Foundation under Grant No. 0400866, the Multi-University Research Initiative, and the Air Force Office of Scientific Research. H.M. and S.H. thank the Alexander von Humboldt Foundation.

-
- [1] A.D. Cronin, J. Schmiedmayer, and D.E. Pritchard, arXiv:0712.3703v1
- [2] H. Müller *et al.*, Phys. Rev. Lett. **100**, 031101 (2008).
- [3] D.S. Weiss, B.C. Young, and S. Chu, Phys. Rev. Lett. **70**, 2706 (1993); M. Weitz, B.C. Young, and S. Chu, *ibid.* **73**, 2563 (1994).
- [4] A. Wicht *et al.*, Physica Scripta **T102**, 82 (2002).
- [5] P. Cladé *et al.*, Phys. Rev. Lett. **96**, 033001 (2006); Phys. Rev. A **74**, 052109 (2006).
- [6] A. Peters, K.Y. Chung, and S. Chu, Nature (London) **400**, 849 (1999).
- [7] M.J. Snadden *et al.*, Phys. Rev. Lett. **81**, 971 (1998).
- [8] T.L. Gustavson, A. Landragin, and M.A. Kasevich, Class. Quantum Gravity **17**, 2385 (2000).
- [9] J.B. Fixler *et al.*, Science **315**, 74 (2007).
- [10] S. Dimopoulos *et al.*, Phys. Rev. Lett. **98**, 111102 (2007).
- [11] H. Müller *et al.*, Appl. Phys. B **84**, 633 (2006).
- [12] S. Dimopoulos *et al.*, arXiv:0712.1250.
- [13] J.M. McGuirk, M.J. Snadden, and M.A. Kasevich, Phys. Rev. Lett. **85**, 4498 (2000).
- [14] S. Gupta, *et al.*, Phys. Rev. Lett. **89**, 140401 (2002).
- [15] D.M. Giltner, R.W. McGowan, and S.A. Lee, Phys. Rev. Lett. **75**, 2638 (1995); Phys. Rev. A **52**, 3966 (1995).
- [16] A. Miffre *et al.*, Eur. Phys. J. D **33**, 99 (2005).
- [17] A.E.A. Koolen *et al.*, Phys. Rev. A **65**, 041601(R) (2002).
- [18] T.W. Hänsch and B. Couillaud, Opt. Commun. **35**, 441 (1980).
- [19] H. Müller, S.-w. Chiow, and S. Chu, Phys. Rev. A **77**, 023609 (2008).
- [20] This relation holds for long pulse durations, but overestimates Ω_{eff} at the short durations used by us [19].
- [21] Y.H. Cha *et al.*, Appl. Opt. A **44**, 7810 (2005).
- [22] H. Müller *et al.*, Opt. Lett. **31**, 202 (2006).
- [23] H. Müller, Rev. Sci. Instr. **76**, 084701 (2005).
- [24] P.J. Mohr and B.N. Taylor, Rev. Mod. Phys. **77**, 1 (2005); P.J. Mohr, B.N. Taylor, and D.B. Newell, arXiv:0801.0028v1 (2007).
- [25] H. Müller *et al.*, Opt. Lett. **30**, 3323 (2005).
- [26] G. Gabrielse *et al.*, Phys. Rev. Lett. **97**, 030802 (2006); *ibid.* **99**, 039902 (2007); D. Hanneke, S. Fogwell, and G. Gabrielse, Phys. Rev. Lett. **100**, 120801 (2008).